

TARGETING BRD4 IN THE TREATMENT OF PLEURAL FIBROSIS

by

JOY ADEWUMI

A thesis submitted in partial fulfillment of
the requirements for the degree of
Master of Science in Biotechnology
Department of Cellular and Molecular Biology

Guoqing Qian Ph.D., Thesis Advisor

School of Medicine

The University of Texas at Tyler
April 2023

The University of Texas at Tyler
Tyler, Texas

This is to certify that the Master's Thesis of

JOY ADEWUMI

has been approved for the thesis requirement on
04/27/2023 for
the Master of Science in Biotechnology degree

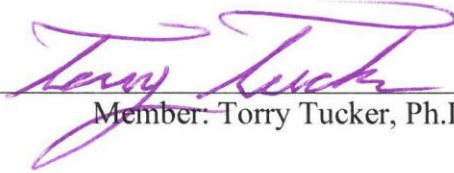
Approvals:



Thesis Chair: Mitsuo Ikebe, Ph.D.



Thesis Advisor: Guoqing Qian, Ph.D.



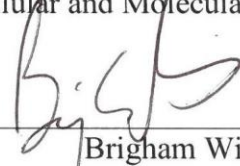
Member: Torry Tucker, Ph.D.



Member: Xia Guo, Ph.D.



Mitsuo Ikebe, Ph.D.
Chair, Department of Cellular and Molecular Biology



Brigham Willis, M.D.
Dean, School of Medicine

ACKNOWLEDGMENTS

I would like to acknowledge my thesis advisor, Dr. Guoqing Qian, for his guidance and support throughout this project. Many thanks also to my thesis committee chair, Dr. Mitsuo Ikebe, and my thesis committee members, Dr. Torry Tucker and Dr. Xia Guo for never hesitating to share their wealth of knowledge and providing all the assistance I needed during this thesis. I also appreciate the time and comments from Dr. Shih-Feng Chou. Your contributions and help have made this thesis a success.

To all the lab members, Dr. Oluwaseun Adeyanju, Dr. Ayobami Olajuyin, Dr. Kiran Kumar, Felix Kankam, and Sana Petkar Khan, I would like to say a big thank you for your indispensable contribution, help, and advice throughout my project.

Thank you all.

TABLE OF CONTENTS

TABLE OF CONTENTS.....	i
LIST OF FIGURES	ii
LIST OF TABLES	iii
LIST OF ABBREVIATIONS.....	iv
ABSTRACT	v
INTRODUCTION.....	1
RESEARCH HYPOTHESIS	10
MATERIALS AND METHODS	11
<i>Reagents and Antibodies</i>	11
<i>HPMC Cell Culture and Treatment</i>	12
<i>Western Blotting</i>	13
<i>Western Blotting Gel Preparation</i>	13
<i>Reverse Transcriptase Polymerase Chain reaction</i>	14
<i>Quantitative Real-Time PCR</i>	16
<i>Gene Silencing with Small Interfering RNA (siRNA) Transfection</i>	17
<i>BRD4 Inhibition Studies</i>	18
<i>Immunohistochemical Staining</i>	19
<i>Statistical Analysis</i>	20
RESULTS	21
<i>The Induction of BRD4 By TGF-B in Primary HPMCs</i>	21
<i>The Requirement of BRD4 in TGF-β-induced MesoMT in Primary HPMCs.</i>	23
<i>The Effects of Pharmaceutical Inhibition of BRD4 in MesoMT Induced by TGF-β</i>	24
<i>Expression of BRD4 in Preclinical Models of PF</i>	29
DISCUSSION	30
REFERENCES.....	36
VITA.....	41

LIST OF FIGURES

Figure 1. Expression of BRD4 and Other MesoMT Markers in TGF- β Dose and Time Course Treatment.....	22
Figure 2. Knockdown of BRD4 Attenuated TGF- β -induced MesoMT in HPMCs.....	23
Figure 3. Effect of Therapeutic Targeting of BRD4 by JQ1 on Expression of MesoMT Markers.....	25
Figure 4. Transcriptional Effect of Therapeutic Targeting of BRD4 on Expression of MesoMT Markers.....	26
Figure 5. Effect of JQ1 on Reversal of Established MesoMT Induced by TGF- β	27
Figure 6. Effect of Therapeutic Targeting of BRD4 by ARV-825 on Expression of BRD4 and MesoMT Markers	28
Figure 7. Representative IHC Staining of BRD4 in PF Induced by <i>S. pneumoniae</i>	29

LIST OF TABLES

Table 1. Stacking and Separating Gel Preparation.....	14
Table 2. Reverse Transcriptase PCR Setup	15
Table 3. Quantitative Real-time PCR Setup.....	16
Table 4: RNA Primers for Quantitative Real-time PCR.....	17

LIST OF ABBREVIATIONS

BET: Bromodomains and extra-terminal

BRD4: Bromodomain-containing protein 4

Col-1: Collagen type I

ECM: Extracellular matrix

FN: Fibronectin

HPMCs: Human pleural mesothelial cells

IHC: Immunohistochemical staining

IPF: Idiopathic pulmonary fibrosis

MesoMT: Mesothelial-to-mesenchymal transition

PBS: Phosphate-buffered saline

PBST: PBS with 0.1% Tween 20

PF: Pleural fibrosis

SDS-PAGE: Sodium dodecyl sulfate-polyacrylamide gel electrophoresis

TGF- β : Transforming growth factor - β

α -SMA: α -Smooth muscle actin

ABSTRACT

Pleural fibrosis (PF) is a respiratory disorder that refers to the thickening and scarring of the pleura. Currently, there is a lack of pharmaceutical treatment options for PF. Pleural mesothelial to mesenchymal transition (MesoMT) is a critical process that contributes to the development of PF. Bromodomain-containing protein 4 (BRD4), a transcriptional and epigenetic regulator, has recently been implicated in a wide range of lung injuries. However, whether BRD4 is involved in regulating MesoMT and the development of PF remains unclear and was explored in this study. Primary human pleural mesothelial cells (HPMCs) were used to test the role of BRD4 in regulating MesoMT. Western blotting and qPCR were conducted to examine protein or mRNA alteration of BRD4 and MesoMT-related markers, such as alpha-smooth muscle actin (α -SMA), collagen type I (Col-1), and fibronectin (FN). Small molecular inhibitors of BRD4 (JQ1 and ARV-825) and small interfering RNA (siRNA) were also employed. We found that BRD4 was induced by TGF- β in HPMCs. Blockade of BRD4 with JQ1 or ARV-825 inhibited TGF- β -induced MesoMT marker expression (α -SMA, Col-1, FN) at both protein and mRNA levels. Consistently, knockdown of BRD4 using siRNA also attenuated MesoMT marker expression (α -SMA, Col-1, FN) induced by TGF- β in HPMCs. In conclusion, BRD4 is involved in MesoMT regulation and may contribute to the development of PF. Future experiments will determine whether BRD4 mediates the induction of MesoMT through the regulation of oxidative stress and the efficacy of targeting BRD4 in the progression of PF induced by *Streptococcus pneumoniae*.

INTRODUCTION

Fibrosis

Fibrosis is a disorder that results from an abnormal wound healing process. Under physiological conditions, tissue injury elicits the transient production of pro-inflammatory mediators and the deposition of excess extracellular matrix (ECM) components. During normal wound healing, the tissue is repaired, and the excess fibrin is resolved by fibrinolysis, thus restoring normal tissue architecture [1]. However, fibrosis occurs during protracted injury due to persistent or severe provocation, which derails the wound healing process causing an unresolved accumulation of ECM. Largely due to the expansion of myofibroblasts and the accumulation of ECM, thickening, and scarring of the affected tissue might occur after a prolonged time [2].

Though it occurs as a result of aberrant wound healing, the onset of fibrosis is heralded by parenchymal cell death resulting from persistent injury. This process leads to inflammatory responses and elicits the production of cytokines and chemokines. These mediators in turn activate key players in this process which are tissue-resident fibroblasts. As severe tissue injury persists, resident fibroblasts undergo phenotypic change and transition to myofibroblasts in a transdifferentiation process known as fibroblast-myofibroblast transition. These mesenchymal myofibroblasts produce and deposit excessive ECM components and are strongly positive for the myofibroblast marker, α -smooth muscle actin (α -SMA). Excessive ECM production by the myofibroblast

population causes prolonged tissue scarring and thickening which leads to tissue damage and reorganization [1].

The outcome of fibrosis is not limited to tissue reorganization and disruption of the normal architecture but could eventually lead to loss of function in affected organs such as the liver, lungs, kidneys, and skin if left unattended. Fibrosis has a high morbidity and mortality rate and has been implicated in about 45% of deaths in the United States in the past two decades [3].

In the case of the lung, the most common and lethal occurrence of fibrosis is idiopathic pulmonary fibrosis (IPF). IPF is a progressive and terminal disorder that involves the scarring and pathological reorganization of the lung interstitium. This is an age-related disease that has a high morbidity that results in difficulty in breathing and eventually, loss of lung function. While IPF has been studied extensively, there is no established cure for this disorder [4]. However, other forms of fibrosis can occur in the lung compartment. One such condition is pleural fibrosis. While not as common or widely studied as IPF, it has been shown to be a significant health concern.

Pleural Fibrosis

Pleural fibrosis (PF) is a respiratory disorder that involves the thickening and scarring of the pleural lining as a result of inflammation in the pleural space. This inflammation can be caused by a variety of processes including exposure to asbestos and immunologic diseases, such as rheumatoid pleurisy, hemorrhagic effusion, bacterial empyema, tuberculosis effusion, malignancy, uremic effusion, or post-coronary artery

bypass graft [5]. The pathogenesis of PF is complex. It involves different types of cells including resident pleural mesothelial cells (PMCs), infiltrating immune cells, and fibroblasts. The progression of PF implicates the inflammation and activation of PMCs.

PF is also associated with increased fibrin deposition resulting from the downregulation of fibrinolysis. The upregulation of PAI-1 suppresses fibrinolysis, which in part contributes to the remodeling of the pleural space [6]. This deposition of the matrix components is determined by the response of mesothelial cells in the pleural lining to injuries caused by the processes earlier mentioned, and their ability to maintain the integrity of the pleural membrane [7]. The balance between progressive fibrosis and the effective resolution of fibrosis is complex and remains incompletely understood.

Mesothelial to Mesenchymal Transition

Mesothelial cells are specialized cells found in an extensive monolayer (the mesothelium) lining the internal organs and serous cavities of the body [8]. Pleural mesothelial cells are pavement-like cells that are metabolically active and are the most common in pleural space. They play key roles in the development of the lungs as they serve as precursors for the endothelial and smooth muscle cells in the pleural space via epithelial-mesenchymal transition [9]. These metabolically active PMCs are also responsible for maintaining homeostatic balance within the pleura, for example, through the production of tissue factor [10]. They create a balance between the hydrostatic and oncotic pressure which affects the morphology of the mesothelium. PMCs have been identified as the central components of immune responses in the pleura. However, PMCs

have also been implicated as key players in the pathogenesis of PF. PMCs play an active role in fibrin deposition at the initial stage of PF as initiated by the coagulation mediator, tissue factor. They also serve as a significant source of collagen which contributes to the scarring associated with PF [6].

As with most types of fibrosis, PF is also characterized by the increased number of α -SMA positive mesenchymal cells and the excessive deposition of ECM in the pleural layer. The increased thickness and deposition of ECM restrict the expansion and mobility of the lung [11]. The involvement of PMCs in the pathophysiology of PF is explained largely by a process termed mesothelial-to-mesenchymal transition (MesoMT). Pleural MesoMT is a process by which PMCs undergo profibrotic phenotypic changes from their normal cobblestone-like morphology to the more spindle-like myofibroblasts. Myofibroblasts are characterized by the expression of α -SMA and increased production of ECM proteins, including collagen and fibronectin (FN). The phenotypic changes observed are also characterized by distinct changes in the cytoskeleton [12], which have been implicated in the reorganization or thickening of the pleura [13, 14].

Transforming Growth Factor- β

Transforming growth factor- β (TGF- β), alongside the likes of thrombin and plasmin have been found to induce MesoMT [15]. TGF- β is a profibrotic cytokine that is considered the most potent inducer of MesoMT and consequently enhances the expression and deposition of collagen in the pleural space. TGF- β also enhances the expression of FN, a scaffold for the deposition of ECM [5, 11]. These processes

collectively contribute to pleural thickening, which is required for the restrictive fibrotic process.

TGF- β signaling in fibroblast to myofibroblast differentiation occurs through the Smad signaling pathway as well as some non-Smad pathways. TGF- β , a dimeric cytokine produced during cellular inflammatory response to tissue injury, binds the type II TGF- β receptor (T β RII), leading to the recruitment and activation of the ALK5, the type I TGF- β receptor. ALK5 phosphorylates receptor-activated Smads, Smad 2/3, which in turn forms a complex with Smad 4. Non-Smad pathways such as the phosphatidylinositol-3-kinase (PI3K), extracellular signal-regulated kinases (ERK), p38, C-Jun N-terminal kinase (JNK), protein kinase-C (PKC δ) and c-AbI pathways are also activated by TGF- β . These TGF- β -activated Smad and non-Smad pathways regulate the transcription and expression of TGF- β target genes such as Snail, Slug, Twist, ZEB, α -SMA, FN, collagen type I (Col-1), tissue inhibitors of metalloproteinases (TIMPs), and matrix metalloproteinases (MMPs) in myofibroblasts, the progression of MesoMT and the onset of tissue fibrosis [16].

Other inducers include tissue factor-dependent extrinsic pathway coagulation factors, factor Xa, and thrombin, which are responsible largely for the initiation of neomatrix formation in the pleural space [5]. These procoagulants and profibrotic mediators are responsible for the conversion of fibrinogen to fibrin and have been shown to induce PAI-1, α -SMA, and Col-1 in PMCs when administered in a concentration-dependent manner [17]. Thrombin and plasmin have also been found to be potent inducers of pleural MesoMT, [15]. Also worthy of mention among these inducers is

urokinase plasminogen activator (uPA) which has been observed to be upregulated in TGF- β mediated MesoMT and has been shown to block or attenuate TGF- β -mediated MesoMT when knocked down by small interfering RNA (siRNA) [13].

Current Treatment of Pleural Fibrosis and Preclinical Studies

Current treatment options for PF include intrapleural fibrinolytic therapy [6], which focuses on increasing fibrinolysis to promote the dissolution of the fibrin neomatrix. However, this therapeutic approach is limited to the treatment of pleural loculations, it does not address tissue reorganization that is caused by inflammation and protracted wound healing.

Recent preclinical studies have identified several novel mediators which may serve as therapeutic targets in the progression of PF. These include glycogen synthase kinase (GSK)-3 β , NADPH oxidase 1 (NOX1), myocardin, $\alpha\beta$ crystallin, endothelial protein C receptor (EPCR), caveolin scanning peptide seven amino acid deletion fragment, mechanistic target of rapamycin (mTOR), and dedicator of cytokinesis 2 (DOCK2) [6]. Recently, Qian et al identified DOCK2 as a mediator of PF via mediating MesoMT process and showed a significant elevation and colocalization of DOCK2 and α -SMA (the MesoMT marker) in the pleura of patients with nonspecific pleuritis and three different preclinical PF models (TGF- β , carbon black/bleomycin, and streptococcal empyema) [18].

Bromodomain-containing Protein 4 (BRD4)

The subject of this proposal is another novel mediator of tissue fibrosis currently

garnering attention, BRD4. BRD4 is a transcriptional and epigenetic regulator [19], which is a bromodomain-carrying member of the Bromodomains and Extra-terminal domains (BET) family. It recognizes and binds acetylated lysine residues on target histone proteins [20]. It has also been shown to play major roles in embryogenesis [21] and cancer development [22] amongst others. BRD4 is of particular interest in diverse forms of tissue fibrosis including idiopathic pulmonary fibrosis, due to its role in mediating profibrotic signaling pathways such as the NF- κ B pathway [23] and Smad pathways [24] through binding to a promoter, enhancer, or super-enhancer.

The BET family consists of four proteins in humans, BRD2, BRD3, and BRD4, found in most tissues, and BRDT found exclusively in the testes. Each of the BET proteins contains two N-terminal bromodomains (BD) and an extra-terminal domain (ET). A C-terminal module (CTM) is also found in BRD4 and BRDT but not in BRD2 or BRD3 [25].

BRD4 is of particular interest because it has been shown to mediate profibrotic gene expression in different tissues [24]. Chromatin structure is highly regulated by histone acetylation of lysine and any disruption of this process could lead to several disorders. Because this process regulates the accessibility of genes to the transcription machinery, it is tightly controlled and is recognized specifically by epigenetic readers such as the members of the BET family like BRD4 [26]. BRD4, recruited by TGF- β at the onset of an injury, regulates lineage-specific and signal-dependent transcription by controlling protein interactions in regulatory regions of the DNA, such as the enhancers and promoters that regulate transcriptional processes responsible for the expression of

profibrotic genes such as inflammatory cytokines [24, 25].

Pharmaceutical Inhibition of BRD4

BRD4 has been explored as a therapeutic target in the attenuation of various forms of lung injuries and tissue fibrosis. This targeting is done via pharmaceutical inhibition of BRD4 by BET inhibitors which prevent the interaction of BRD4 with transcriptional regulators of profibrotic gene expression [24].

Small molecule BET inhibitors such as BRD4-targeting JQ1 have a high binding affinity for the acetyl-lysine recognition pocket of BRD4 such that they can competitively displace BRD4 and inhibit its interaction with acetylated lysine residues at the regulatory sites of target genes [27]. Others include proteolysis targeting chimeras (PROTACs), which induce selective intracellular proteolysis. The PROTAC consists of a ligand of the target protein, such as a small-molecule inhibitor of BET proteins, which is covalently linked to a ubiquitin ligase system, such as E3 ubiquitin ligase. It acts by binding the target protein using the ligand moiety and recruits the ubiquitin ligase for targeted ubiquitination of the bound target protein through the ubiquitin-mediated proteasomal degradation system [28]. An example of this BRD4-targeting PROTAC is ARV-825, which has been investigated in the pharmaceutical inhibition of BRD4 in various types of cancers [29, 30].

The pharmaceutical inhibition of BRD4 has been employed in various forms of tissue fibrosis as a potential therapeutic option. An example is TGF- β -induced cardiac fibrosis where JQ1-inhibition of BRD4 resulted in attenuation of transverse aortic

constriction-induced cardiac fibrosis [31]. In carbon tetrachloride-induced liver fibrosis in mouse models, JQ1 treatment was shown to reverse fibrotic response in hepatic stellate cells [32]. JQ1 and ARV-825 blockade of BRD4 also produced antifibrotic response in patient-derived diffuse cutaneous systemic sclerosis fibroblasts [33]. I-BET151 inhibition of BRD4 inhibited renal fibroblast activation and attenuated renal fibrosis in a murine model of renal fibrosis induced by unilateral ureteral obstruction [34].

In various forms of lung injuries, the therapeutic targeting of BRD4 has also been explored. In sepsis-induced lung injury, the progression of the disease was inhibited via the suppression of BRD4 [35]. In lung fibrosis, the resolution of the disease was accelerated via the downregulation of the oxidant-generating enzyme, NOX4 via inhibition of BRD4 [36]. In acute respiratory syndrome, the disease was attenuated by the nanotherapy targeting of BRD4 [37]. In airway remodeling, treatment was performed via the therapeutic targeting of BRD4 [38]. In pulmonary fibrosis, inhibition of BRD4 via the administration of therapeutic doses of JQ1 and the BET inhibitor CG223 showed significant attenuation in profibrotic responses in lung fibroblasts of patients with rapidly progressing idiopathic pulmonary fibrosis and bleomycin-induced pulmonary fibrosis model, respectively [39, 40].

Despite its significance in the pathogenesis of lung injuries, there is a lack of research to show the role of BRD4 in the development of PF. PF is associated with chronic inflammation and oxidative stress is proposed as an important mechanism for the progression of PF. For example, NOX1 was found to promote MesoMT through ROS signaling, however, its downregulation attenuated MesoMT induction in an *S.*

pneumoniae model of PF[41]. Because BRD4 plays an important role in regulating oxidative stress, inflammation, and cell phenotypic regulation, it is potentially involved in the pathogenesis of PF. Thus, we hypothesize that BRD4 plays an important role in mediating MesoMT to promote PF.

RESEARCH HYPOTHESIS

This study hypothesizes that BRD4 plays an important role in mediating mesothelial-to-mesenchymal transition (MesoMT) to promote PF.

To test this hypothesis, the following objectives will be accomplished:

1. Investigate the induction of BRD4 by TGF- β in primary human pleural mesothelial cells (HPMCs).
2. Investigate the requirement of BRD4 in TGF- β -induced MesoMT in primary HPMCs.
3. Test the effects of pharmaceutical inhibition of BRD4 in pleural MesoMT induced by TGF- β .
4. Determine the expression of BRD4 in preclinical models of PF.

MATERIALS AND METHODS

Reagents and Antibodies

LHC-8 medium and RPMI-640 for cell culture and starvation were purchased from ThermoFisher Scientific and VWR Life Science, respectively. TGF- β -1 for MesoMT induction was purchased from R&D systems. JQ1 small molecule inhibitor and PROTAC, ARV-825 were obtained from MedChemExpress.

Trizol, isopropanol, chloroform, and glycogen used in RNA extraction were obtained from Sigma Aldrich. The iScript cDNA synthesis kit was obtained from Bio-Rad. The SYBR green and RNA primers used in the analysis of gene expression were also purchased from Bio-Rad and Integrated DNA Technologies, respectively.

The jetPRIME transfection reagent and siRNA used for the transfection procedure were obtained from Polypus-transfection and Sigma Aldrich, respectively.

The lysis buffer, protease, and phosphatase inhibitors for cell collection and the BCA protein assay kit for protein concentration determination were all purchased from ThermoFisher Scientific.

For gel preparation and electrophoresis, the apparatus was obtained from Bio-Rad. The reagents include glycerol and ammonium persulfate (APS) from Sigma Aldrich, Tris-HCl buffers from Bio-Rad, ethanol from KOPTEC, and SDS from Thermo Fisher Scientific. The acrylamide used was from Ambion Inc., and TEMED was from Invitrogen. The running buffer for SDS-PAGE was made from 10x Tris-Glycine SDS solution purchased from ThermoFisher Scientific. The transfer buffer was made from

glycine purchased from Research Products International, tris-base purchased from Thermo Fisher Scientific, and ethanol from KOPTEC. PBST was made from PBS and 0.1% Tween 20 and both were purchased from ThermoFisher Scientific.

The FN, Col-1, α -SMA, BRD4, and GAPDH primary antibodies used to probe the markers during western blotting were purchased from Abcam. The FN antibody was specific for all three isoforms of FN. Milk and BSA used for blocking during western blotting were purchased from Research Products International and Thermo Fisher Scientific, respectively. Stripping buffer for stripping PVDF membranes was bought from EMD Millipore Corporation.

The IHC primary antibody and HRP secondary antibody were purchased from Cell Signaling Technologies and ThermoFisher Scientific, respectively. The IHC DAB staining kit was obtained from Vector Labs.

HPMC Cell Culture and Treatment

Primary human pleural mesothelial cells (HPMCs) were cultured in LHC-8 medium supplemented with 3% FBS, 2% antibiotic-antimycotic, and 1% GlutaMAX in a humidified incubator at 37°C with 5% CO₂. HPMCs were serum-starved in serum-free RPMI-1640 medium supplemented with GlutaMAX and were treated with recombinant human TGF- β either at a conventional dose of 5 ng/mL or in a time-dependent manner (0, 2, 4, 8, 24, and 48 hours). The 0 ng/mL and 0-hour treatments are negative controls where TGF- β is not administered.

Western Blotting

Whole-cell lysates were collected from primary HPMCs following different treatments as indicated in experiments in radioimmunoprecipitation assay (RIPA) lysis buffer with protease and phosphatase inhibitors. The samples were lysed with gentle rotation for 40 minutes at 4°C and then centrifuged for 15 minutes at 13,000 rpm at 4°C. The supernatant was collected into 1.5 mL Eppendorf tubes and total protein concentration was determined using the bicinchoninic acid (BCA) protein assay kit, according to the manufacturer's manual. The protein concentration was measured using the TECAN INFINITE M PLEX plate reader.

Equal amounts of the total protein were denatured using the Laemmli SDS buffer and were loaded for SDS-PAGE gel electrophoresis at 90V for the first 20 minutes and 120V for the rest of the run till the protein had sufficiently run down the gel. The proteins were transferred to PVDF membranes using a transfer system at 150 V for 2.5 hours. The PVDF membranes were then blocked with 3% BSA in PBST, and incubated with primary antibodies against BRD4, α -SMA, Col-1, and FN, respectively, at 4°C overnight. GAPDH was used as the loading control.

Western Blotting Gel Preparation

The separating gels used for protein detection were prepared at 8% concentration. Glass plates were set up on a specially designed gel-casting stand. Using the formula in the table below, the separating gel was prepared first in a 50 mL tube and 7.2 mL is transferred into the glass plates and topped with 1 mL of 100% ethanol to level the gel

and remove bubbles. After 25 minutes when the gel became solid, the ethanol was poured out and the remnant was allowed to evaporate completely. The stacking gel was also prepared in a 50 mL tube using the formula in the table below. The stacking gel was added to the gel-casting apparatus to the brim after which a 10-well comb was carefully inserted into the slot without introducing bubbles. After the gel solidified in about 30 minutes, it was removed from the stand and wrapped in a water-soaked paper towel and stored at 4°C and used within a few days.

8% Separating Gel Reagents	Total Volume (7.5 mL)	5% Stacking Gel Reagents	Total Volume (4 mL)
H ₂ O	2.6 mL	H ₂ O	2.42 mL
40% Acrylamide	1.4 mL	40% Acrylamide	0.5 mL
Tris-HCl 1.5 M (pH 8.8)	1.9 mL	Tris-HCl 0.5 M (pH 8.8)	1 mL
50% Glycerol	1.5 mL	10% SDS	40 uL
10% SDS	75 uL	10% APS	40 uL
10% APS	75 uL	TEMED	4 uL
TEMED	3 uL		

Table 1: Separating and Stacking Gel Preparation

Reverse Transcriptase Polymerase Chain reaction

RNA Preparation

The cells were lysed with 1 mL of Trizol reagent per well of a 6-well culture dish. The lysates were incubated in Trizol for 5 minutes at room temperature after which they were collected into 1.5 mL Eppendorf tubes. Afterward, 0.2 mL of chloroform was added to each tube and the caps were tightly secured. The tubes were shaken vigorously by hand

for 15 seconds, twice, after which they were incubated at room temperature for 3 minutes.

The samples were centrifuged at 12,000 g for 15 minutes at 4°C. Afterward, the colorless upper aqueous phase was transferred to fresh tubes. To precipitate the RNA from the aqueous phase, 0.5 mL of isopropyl alcohol (kept cool at 4°C) and 1 µL of glycogen were added to the aqueous phase. The samples were mixed well and incubated at -20°C for 30 minutes after which they were centrifuged at 12,000 g for 20 minutes at 4°C. The supernatant was removed by careful decanting. RNA precipitate formed a gel-like pellet on the side and bottom of the tube.

The pellets were washed with 1 mL of 75% ethanol (prepared using autoclaved diH₂O). The samples were mixed by inverting the tubes and centrifuging at 12,000 g for 10 minutes at 4°C. The supernatant was removed by carefully pipetting and the RNA pellets were air-dried for 5 minutes. The RNA pellets were dissolved in 20 µL of DEPC water and were incubated at 60°C for 10 minutes. Afterward, the RNA concentration was detected using the TECAN INFINITE M PLEX plate reader.

Reverse Transcriptase PCR

The RT-PCR was set up in 1.5 mL Eppendorf tubes using the following formula:

Reverse Transcriptase PCR Reaction System (20 µL)	Volume (µL)
5x iScript Reaction Mix	4
iScript Reverse Transcriptase	1
Denatured RNA template	X
RNase-free water	(15-x)

Table 2: Reverse Transcriptase PCR Setup

The volume of the RNA template (x) is determined from the RNA concentration determination and is the volume of 1 μg of the RNA template. Afterward, the reverse transcriptase reaction is run on the BIORAD C1000 Touch Thermal Cycler to convert the RNA template to cDNA using the following protocol.

Quantitative Real-Time PCR

The cDNA samples from the RT PCR process are diluted with 40 μL of nuclease-free water after which they are prepared for the qRT PCR procedure. A master mix (for each target gene) was prepared using the 2X SYBR Green Supermix, the diluted cDNA template, and nuclease-free water, using the formula below. For each target gene, there are n reactions depending on the treatment conditions.

qRT-PCR reaction system (10 μL)	n reactions (μL)
Nuclease-free water	3.5 x (n+1)
2X SYBR Green Supermix	5 x (n+1)
Diluted cDNA template	0.5 x (n+1)
Primers (F+R, 5 μM)	1

Table 3: Quantitative Real-time PCR Setup

Aliquots of 9 μL were transferred into designated wells in a 96-well PCR plate after which forward (F) plus reverse (R) primers were added individually for BRD4, α -SMA, Col-1, and FN target genes to the appropriate wells.

BRD4	Forward	5'-CGCTATGTCACCTCCTGTTTGC-3'
	Reverse	5'-ACTCTGAGGACGAGAAGCCCTT-3'
α -SMA	Forward	5'-GCCCTGGATTTTGAGAATGA-3'
	Reverse	5'-ATGCCAGCAGATTCCATAACC-3'
Col-1	Forward	5'-GAACGCGTGTTCATCCCTTGT-3'
	Reverse	5'-GAACGAGGTAGTCTTTCAGCAACA-3'
FN	Forward	5'-CAAACCTACGGATGACTCGT-3'
	Reverse	5'-GCTCATCATCTGGCCATTTT-3'
GAPDH	Forward	5'-TGCACCACCAACTGCTTA-3'
	Reverse	5'-GGATGCAGGGATGATGTTC-3'

Table 4: RNA Primers for Quantitative Real-time PCR

The plate was sealed using PCR-grade sealing films. The plates were centrifuged at 1000 rpm for 2 minutes at room temperature. The qPCR was run using the BIORAD CFX96 qPCR machine using a pre-defined protocol of 10 μ L reaction, SYBR Green, and no melting curve. The qPCR was run for approximately 1 hour and the data is analyzed. The primers used for BRD4, α -SMA, Col-1, and FN were as below:

Gene Silencing with Small Interfering RNA (siRNA) Transfection

HPMCs were transfected with 10 ng/mL of control siRNA and siRNA targeting the BRD4 gene in a 6-well plate, using the jetPRIME transfection reagent according to the manufacturer's guide. The medium in the culture dish was removed and replaced with 2 mL of the LHC-8 transfection medium per well of a 6-well culture dish. Then the transfection solution was prepared by adding 10 μ L of the siRNA or scramble (control) in 200 μ L of the transfection buffer. The solution was vortexed for 15 seconds and spun

down for 5 seconds. Afterward, 10 μ L of the transfection reagent, jetPRIME, was added to the solution after which it was vortexed for 3 seconds and spun down for a second. The solution was incubated at room temperature for 15 minutes, followed by adding dropwise into the designated wells. After gently mixing, the cells were incubated overnight. The cells were then starved in serum-free RPMI-1640 medium for 8 hours, followed by the addition of 5 ng/mL of TGF- β after 24 hours.

BRD4 Inhibition Studies

For BRD4 inhibition studies, blockade and reversal studies were performed. For blockade studies, HPMCs were starved in 2 mL of serum-free medium overnight in a 37°C incubator with 5% CO₂. The cells were pretreated with varying concentrations of the small molecule BET inhibitor JQ1 (0.1, 0.5, 1, and 2 μ M) or BET degrader, ARV-825 (5, 10, 50, and 100 nM). Thirty minutes later, the cells were treated with 5 ng/mL of TGF- β for 24 hours for RNA isolation or 48 hours for protein extraction. Two wells were set up as the negative (without TGF- β) and positive control (with TGF- β , minus the inhibitor), respectively.

For reversal studies, serum-starved HPMCs were treated first with 5 ng/mL of TGF- β for 24 hours, followed by treatment with JQ1 using the same dosage as the blockade studies. The cells were then incubated at 37°C in a CO₂-hooked incubator and collected after 48 hours for protein expression detection. The cells were afterward collected for protein expression analyses using Western blotting.

Immunohistochemical Staining

Pleural tissues were collected from mice challenged with *Streptococcus pneumoniae* (*Strep*) and saline-treated control mice. After collection, freshly dissected tissues were fixed with 4% paraformaldehyde and dehydrated in increasing concentrations of alcohol (50% to 100%). The tissues were then cleared in xylene and embedded in a paraffin block and sectioned at 5 µm in a microtome and transferred to glass slides suitable for immunochemistry.

The paraffinized tissue sections were deparaffinized in xylene and then hydrated in decreasing concentrations of alcohol (100% to 50%) and afterward in distilled water. An antigen retrieval was performed to unmask the antigenic epitope using Tris-EDTA buffer after which an Immedge pen was used to draw a circle around the edges of the tissue sections on the glass slides. Endogenous peroxidase activity was blocked by incubating the tissue sections in freshly prepared 3% H₂O₂ solution in methanol at RT in a humidified chamber.

Blocking was done using 10% goat serum in 0.1% triton X-100 in the humidified chamber at RT. Following that, BRD4 primary antibody was added to the sections and incubated in the humidified chamber at 4°C overnight, followed by washing with PBST and incubation with HRP-secondary antibody in a humidifier chamber at RT. DAB substrate was added to the sections to reveal the color of the antibody staining and counterstained by IHC nuclear staining.

For IHC nuclear counterstaining, the tissue sections were immersed in Harris hematoxylin, rinsed, immersed in differentiating solution, rinsed, and finally in bluing solution and rinsed.

Following IHC nuclear staining, the pleural tissue sections were dehydrated in increasing concentrations (95-100%) of alcohol, cleared in xylene, and covered with coverslips using the mounting solution. The color of the BRD4 antibody staining was observed using microscopy to compare the induction of BRD4 in the *Strep* mice model and saline-treated pleural tissue sections.

Statistical Analysis

Western blot data are shown as mean \pm SE. mRNA data are shown as mean \pm SD. Multiple comparisons were done with one-way ANOVA followed by Dunnett's test. P-value less than 0.05 was considered statistically significant.

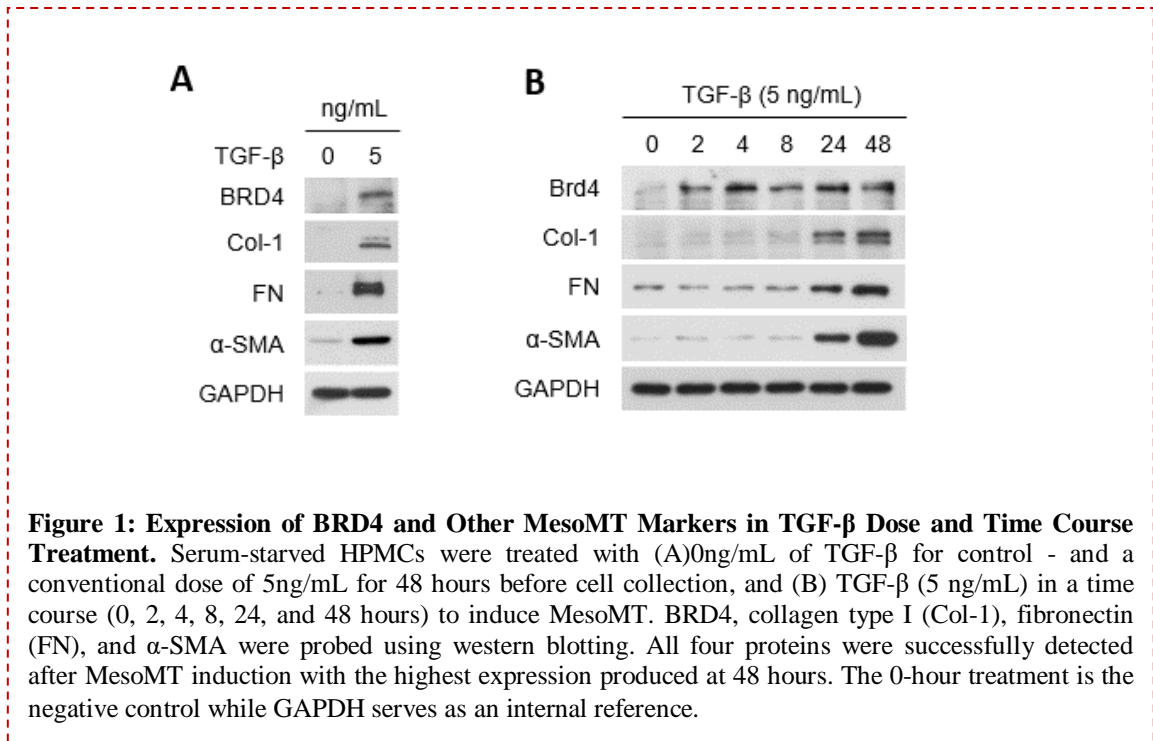
RESULTS

To test the hypothesis that BRD4 plays an important role in mediating MesoMT to promote PF, this study was divided into four major objectives to investigate the role of BRD4 in pleural MesoMT *in vitro* and its induction in a *Strep* model of pleural injury *in vivo*.

The Induction of BRD4 By TGF- β in Primary HPMCs

HPMCs were treated with TGF- β to investigate the induction of BRD4 along with TGF- β -induced MesoMT markers. Figure 1A below presents the induction of BRD4 by TGF- β at 5 ng/mL, while Figure 1B presents the induction of BRD4 in a time course featuring a 0-hour treatment (negative control) where TGF- β was not administered, and 2, 4, 8, 24, and 48-hour treatments. The MesoMT marker α -SMA, and extracellular matrix proteins, FN and Col-1 were also detected, as are established as markers of MesoMT.

BRD4 was induced in the HPMCs treated with 5 ng/mL of TGF- β when compared to the negative control. There was also induction of MesoMT markers, α -SMA, Col-1,



and FN at the same TGF- β dose. There was a notable increase in the expression of Col-1, α -SMA, and FN after 24 hours of treatment with TGF- β and beyond, as indicated by the increase in the intensity of the bands, with the highest expression recorded at the 48-hour treatment. BRD4 expression was induced as well at 2 hours post TGF- β treatment and the induction prolonged over the treatment period of 48 hours. As expected, the non-treatment control group (negative control) showed little or no expression of the MesoMT markers. GAPDH served as the load control. The equal expression of GAPDH across all time points showed that the volume of each sample loaded was equal.

The Requirement of BRD4 in TGF- β -induced MesoMT in Primary HPMCs.

To investigate the requirement of BRD4 in TGF- β -induced MesoMT in HPMCs, the BRD4 gene was silenced using BRD4-targeting siRNAs. Prior to MesoMT induction with TGF- β , the cells were transfected with control siRNA (scramble) and two different BRD4-targeting siRNAs (siBRD4#1 and #2).

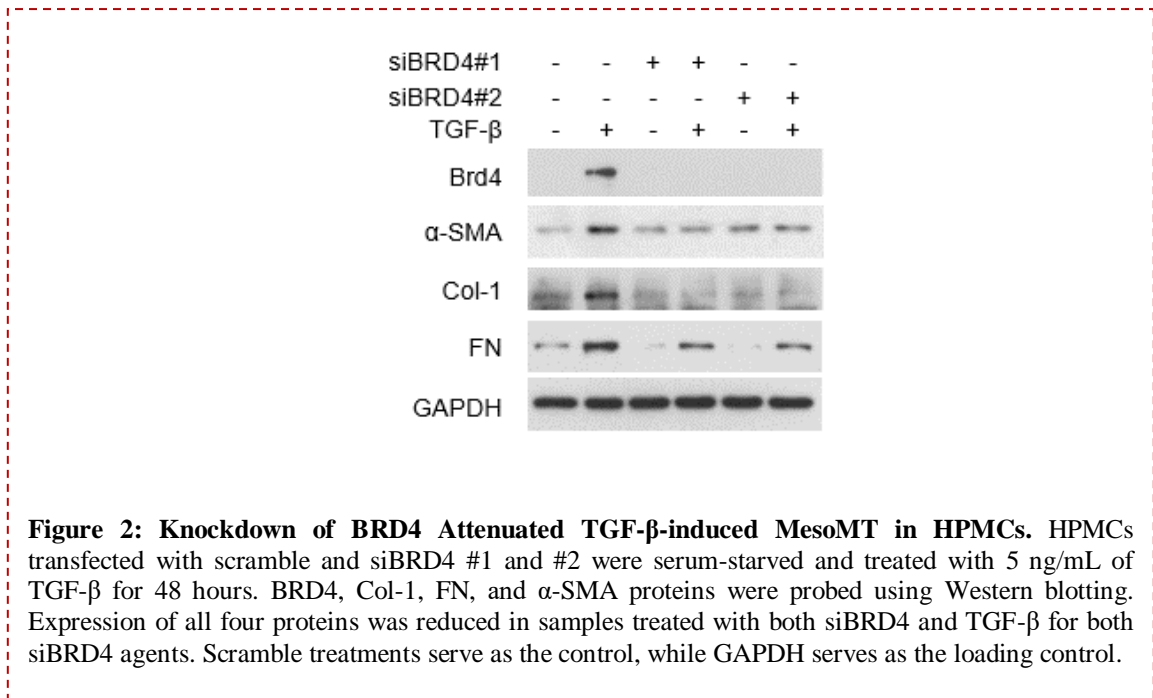


Figure 2 presents the Western blot result of the expression of BRD4, α -SMA, FN, and Col-1 after siBRD4 transfection and TGF- β treatment of serum-starved HPMCs. When compared to the scramble control, there was a pronounced decrease in BRD4 induction after transfection with both siBRD4 #1 and #2 in the presence of TGF- β ,

indicating the successful silencing of the BRD4 gene. BRD4 silencing also attenuated the induction of MesoMT markers, α -SMA, FN, and Col-1. GAPDH was used as the loading control in this experiment.

The Effects of Pharmaceutical Inhibition of BRD4 in MesoMT Induced by TGF- β

The pharmaceutical inhibition of BRD4 was performed using a small molecule BET inhibitor JQ1 and a BET-targeting proteolysis-targeting chimera, ARV-825. The effect of the inhibitor and the PROTAC on the induction of MesoMT by TGF- β was investigated in this aim. Both blockade and reversal studies were performed to assess the effect of JQ1 and ARV-825 on the induction of MesoMT. Blockade studies were performed in serum-starved HPMCs treated with different doses of JQ1 (0.1, 0.5, 1, and 2 μ M) or ARV-825 (5, 10, 50, 100 nM) after which the cells were treated with 5 ng/mL TGF- β , while reverse inhibition studies involved the induction of MesoMT with TGF- β before treatment with JQ1.

Figures 3 and 4 show the Western blot results for the expression of MesoMT markers, α -SMA, FN, and Col-1, in JQ1 blockade studies.

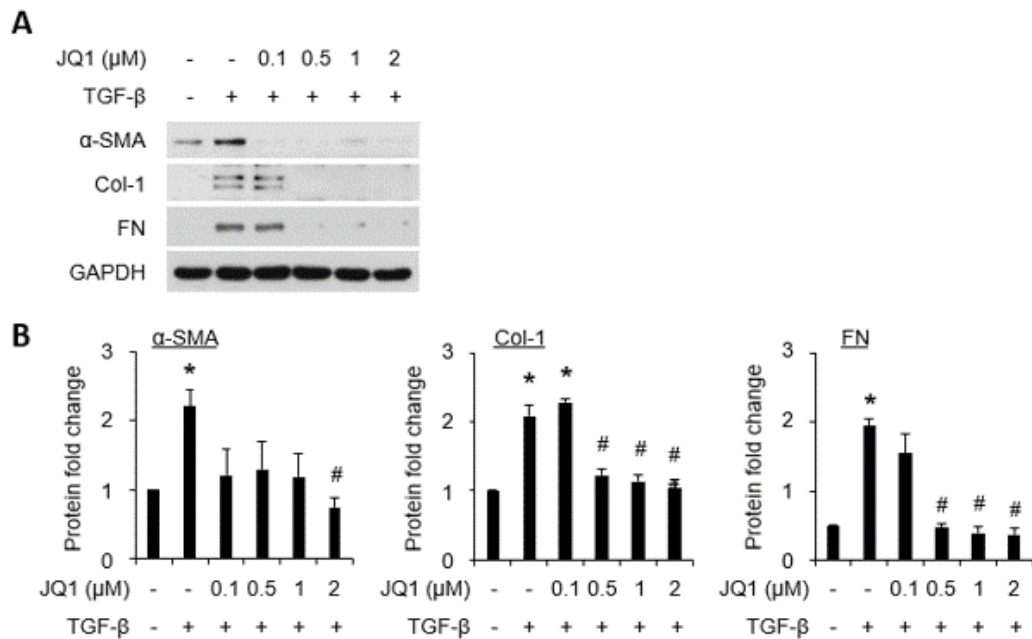
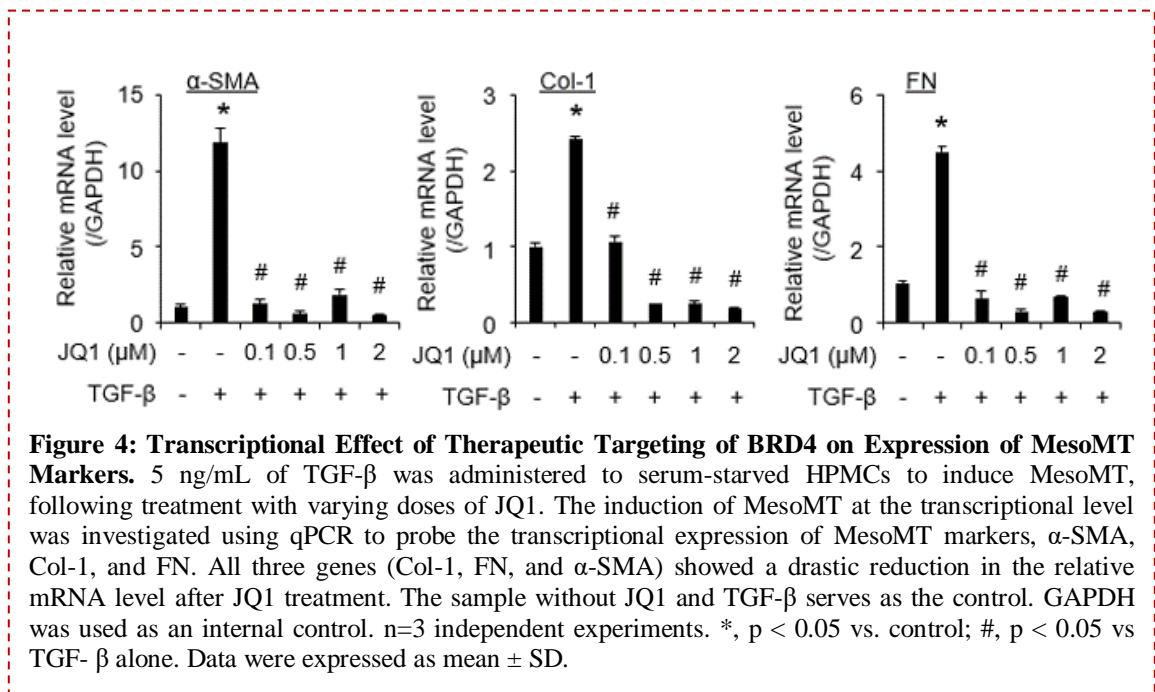


Figure 3: Effect of Therapeutic Targeting of BRD4 by JQ1 on Expression of MesoMT Markers. 5 ng/mL of TGF- β was administered to serum-starved HPMCs to induce MesoMT, following treatment with varying doses of JQ1. Col-1, FN, and α -SMA proteins were probed using (A) western blotting, (B) and quantified using densitometry. All three proteins showed a reduction in protein expression in cells treated with JQ1. The sample without JQ1 and TGF- β treatment is the control while GAPDH serves as an internal reference. n=3 independent experiments. *, p < 0.05 vs. control; #, p < 0.05 vs TGF- β alone. Data were expressed as mean \pm SE.

In the absence of JQ1, TGF- β induced MesoMT markers, α -SMA, Col-1, and FN, however, at low doses of JQ1 (0.1 μM), induction of α -SMA but not Col-1 and FN was inhibited. At higher doses (> 0.1 μM), the induction of all three MesoMT markers was notably attenuated. This effect is confirmed by the densitometry data provided in Figure 3B. For Col-1 and FN, the lowest expression was found to be fairly equal across the three highest doses and significantly lower than the treatment with TGF- β only, while for α -SMA, the highest JQ1 dose, showed a statistically significant reduction in expression.

This is likely due to variation between experiments. GAPDH served as the internal loading control.

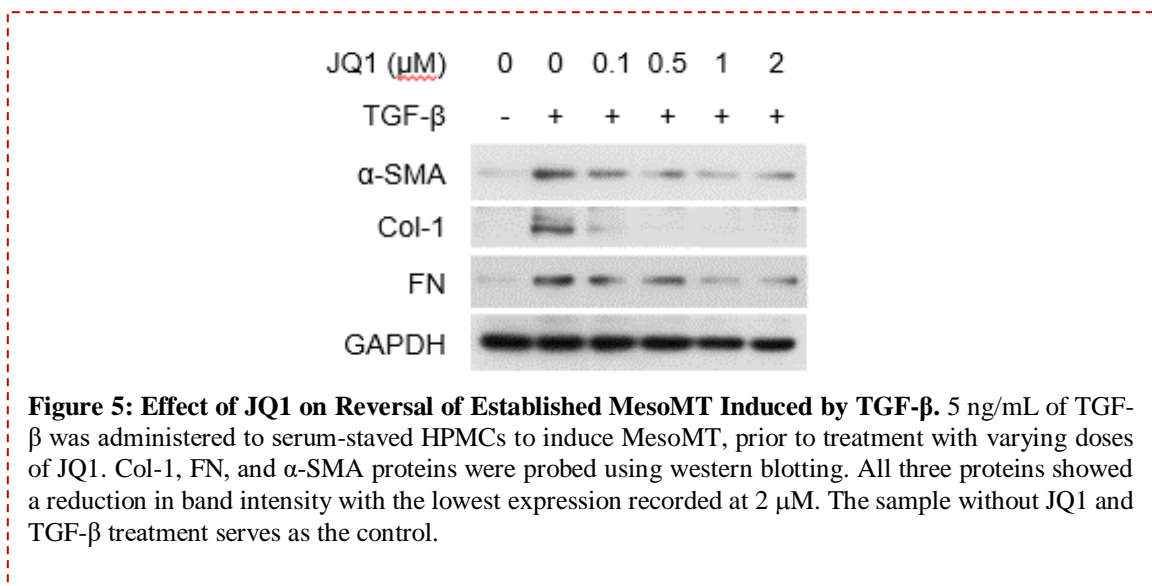
mRNA analysis of the JQ1 blockade was performed to investigate the effect of JQ1 on inhibiting the induction of MesoMT, at the transcriptional level. Figure 4 below presents the results of this analysis.



The mRNA analysis showed a notably high mRNA level relative to the internal reference (GAPDH) for all the MesoMT markers in HPMCs treated with TGF-β only. However, transcription of these markers reduced significantly in HPMCs treated with

JQ1 when compared to the cells with no JQ1 treatment. The reductions in relative mRNA levels observed across the three genes, for all doses of JQ1 administered, were all statistically significant.

Figure 5 below presents the effect of pharmaceutical reverse inhibition of BRD4 on the

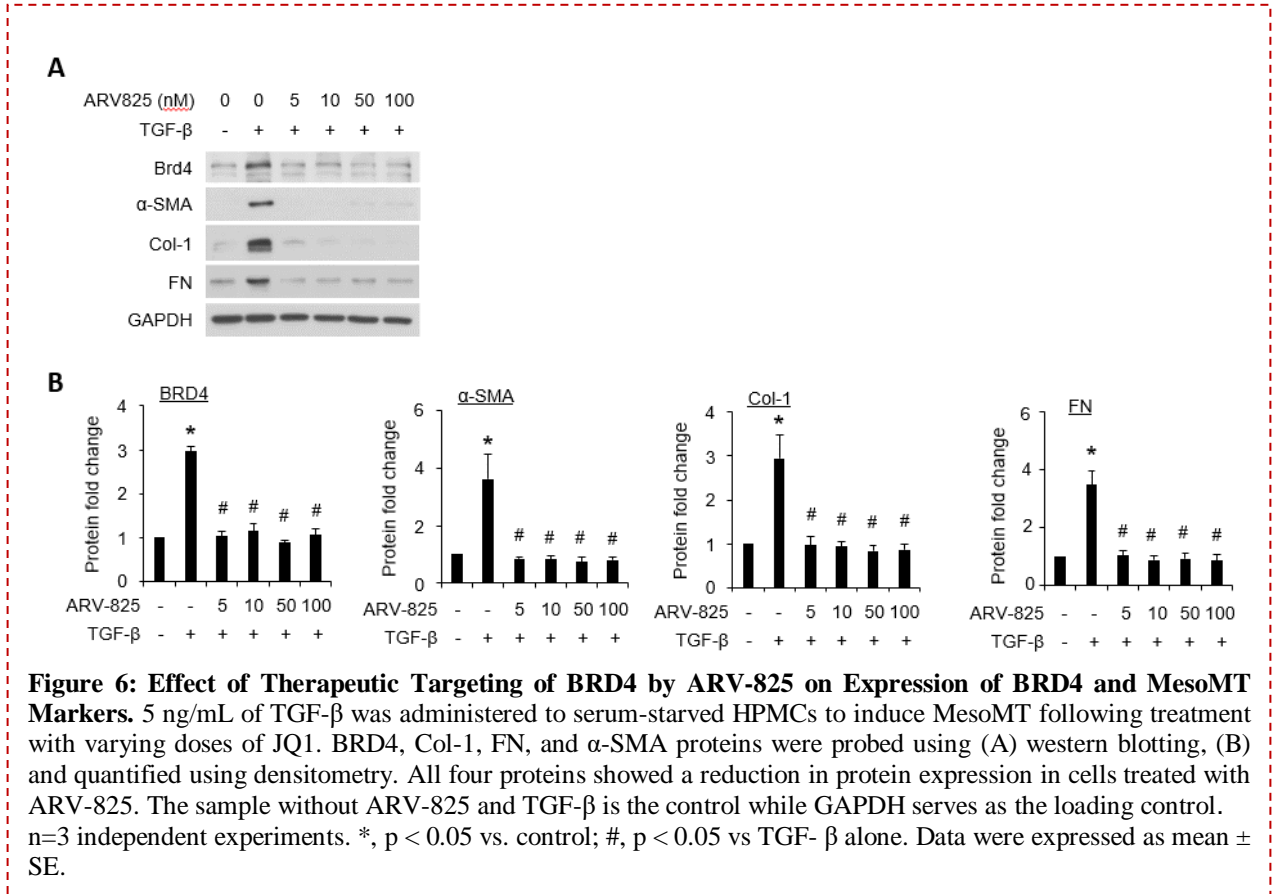


induction of TGF- β -induced MesoMT by JQ1 in HPMCs.

The reversal studies showed some attenuation in the expression of MesoMT markers with the lowest band intensity generally showing at the lowest concentration of JQ1 treatment for all three proteins detected. Inhibition of Col-1 expression was however more profound than the other markers. GAPDH was used as a loading control to confirm equal SDS-PAGE loading.

The effects of the pharmaceutical targeting of BRD4 using BET PROTAC degrader, ARV-825, on the induction of TGF- β -induced MesoMT was also explored.

Figure 6 presents the Western blot results for the expression of BRD4, and MesoMT markers, α -SMA, FN, and Col-1, in ARV-825 blockade studies.

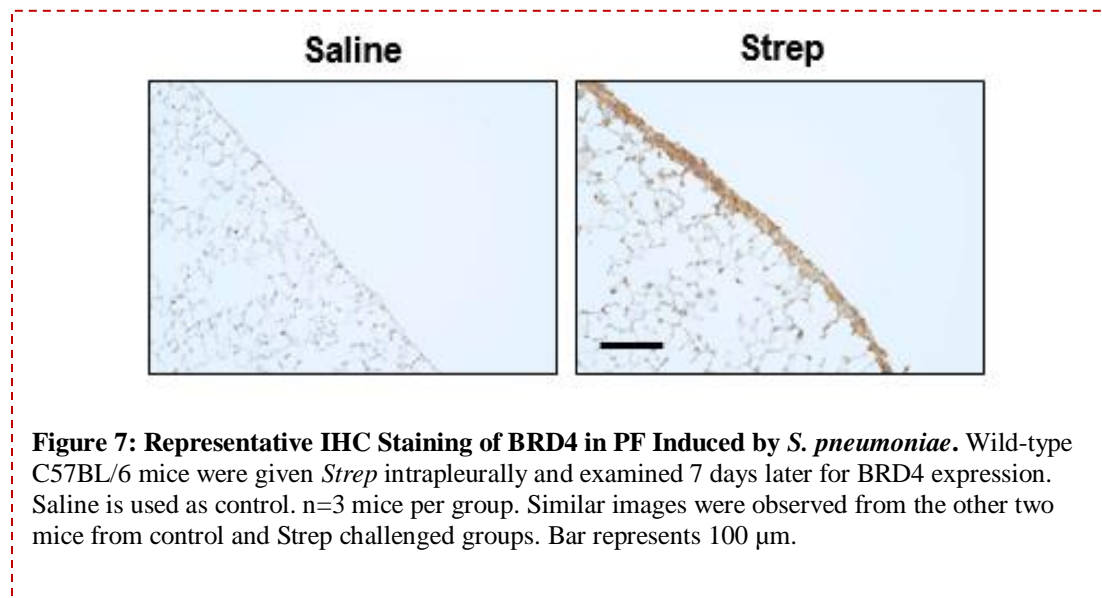


The western blot images in Figure 6A showed a notable induction of BRD4 and all MesoMT markers in HPMCs treated with TGF- β only. Treatment with ARV-825, however, eliminated the induction across all the markers as shown by the reduction in band intensity. The densitometry analysis in Figure 6B confirmed this effect. Across all four proteins, a statistically significant reduction in band intensity was observed in cells treated with ARV-825, from the lowest dose to the highest (5-100 nM), when compared with the cells treated only with TGF- β . GAPDH served as the loading control.

Expression of BRD4 in Preclinical Models of PF

Using immunohistochemical staining, lung tissues obtained from mice treated with *Strep* to induce pleural injury were compared with tissues collected from saline-treated mice to determine the expression of BRD4 in a preclinical model of PF. Figure 7 presents microscopy images for the pleura from both saline and *Strep*-treated mice.

The images showed a thickening of the pleural lining of the lung tissue section



from mice induced with *Strep* while the saline-treated tissue section showed a normal, thin lining. Also, there was a strong brown coloring on the pleural lining of the *Strep*-induced tissue indicating the expression of BRD4 following BRD4 antibody incubation, during the IHC staining. This coloring is not observed in the lining of the saline-treated tissue section.

DISCUSSION

The development and progression of PF is a major health concern, which, like other forms of tissue fibrosis, could lead to organ failure [3]. Current treatment options which are mostly surgical and invasive include intrapleural fibrinolytic therapy which clears the accumulated fibrin neomatrix but does not address the scarring and thickening from the reorganization of the pleural tissue. Thus, recent preclinical studies are geared towards investigating potential therapeutic targets that could reverse tissue reorganization by blocking pleural MesoMT [6]. Accumulating evidence implicates BRD4 in the regulation of different pathological processes including oxidative stress, inflammation, and cell phenotypic regulation, all of which are involved in the pathogenesis of PF. The thesis work aims to explore the role of BRD4 in the regulation of MesoMT using primary HPMCs and its expression in PF.

Our data showed the induction of BRD4 alongside the MesoMT markers, α -SMA, Col-1, and FN (Figure 1A) caused by TGF- β in HPMCs, suggesting the potential involvement of BRD4 in the induction of MesoMT. The increase in BRD4 expression over a time course (Figure 1B) also mimics the trend of the other markers, further reinforcing the suggestion that BRD4, like these other markers, may play a role in the TGF- β -induced MesoMT. A similar heightened BRD4 protein level expression was

reported in western blot images for tissues obtained from liver fibrosis patients [29] and in renal tissues of hypertensive nephropathy patients [42] when compared to normal control groups.

To ascertain that BRD4 is a potential therapeutic target in pleural MesoMT, we investigated its requirement for the induction of pleural MesoMT using BRD4-targeted siRNA. The Western blot data (Figure 2) showed that both siRNAs used blocked the expression and induction of BRD4 by TGF- β . Furthermore, the knockdown of BRD4 suppressed the expression of MesoMT marker α -SMA, Col-1, and FN induced by TGF- β in primary HPMCs. Together, these data suggest that BRD4 plays an important role in TGF- β -induced MesoMT, that is, there is a possibility that when BRD4 translation is disabled, as is with BRD4-targeting siRNA transfection, the induction of MesoMT in the pleural space will be blocked or attenuated. The requirement of BRD4 was demonstrated in hepatic fibrosis where siRNA-mediated depletion of BRD4 was also found to decrease ECM component expression in the presence of TGF- β [32]. Whether BRD4 is also involved in MesoMT induction by other mediators than TGF- β , for example, thrombin and plasminogen, deserves further investigation.

Having confirmed not only the involvement of BRD4 but also its requirement for the induction of pleural MesoMT in HPMCs, we investigated the effect of the pharmaceutical inhibition of BRD4 in HPMCs. Blockade studies using JQ1, a small-molecule inhibitor of BRD4, and ARV-825, a BET-targeting PROTAC, resulted in the successful attenuation of the expression of MesoMT markers, α -SMA, Col-1, and FN, upon induction by TGF- β as shown by Western blot and mRNA data (Figures 3-6).

The blockade studies (Figures 3 and 6) showed statistically significant attenuation in the expression of the markers, mostly in the higher doses of JQ1 (0.5-2 μ M) and in all doses of ARV-825. The protein expression levels observed at these doses were similar to the control without TGF- β or inhibitor treatment. It remains speculative whether JQ1 affects the level of BRD4. Since JQ1 is competitive inhibitor of BRD4, disturbing its binding with acetylated residues, it is not supposed to affect the level of BRD4 directly. Previous reports also show discrepancy, and no mechanism has been mentioned. Some studies show that JQ1 did not affect BRD4 levels [43, 44] while other studies show the opposite, although at higher doses [45]. There seems to be cell-dependent effects. ARV-825, on the other hand, degraded BRD4, thus reducing its protein level significantly. These suggest that the therapeutic targeting of BRD4 blocks the induction of the MesoMT process in HPMCs. mRNA analysis (Figure 4) also revealed that the therapeutic targeting of BRD4 by JQ1 blocks the transcription of MesoMT markers induced by TGF- β in HPMCs. The result suggests that BRD4 inhibition blocks MesoMT induction at the transcriptional level. It is likely that the effect observed at the protein level (Western blots – Figure 3) is a downstream effect of the inhibition at the transcriptional level. In future investigations, we would see if the pharmaceutical targeting of BRD4 by BET-targeting PROTAC, ARV-825 also blocks the induction of MesoMT at the transcriptional level.

The doses used administered for both JQ1 [31, 32, 36] and ARV-825 [46, 47] were referred to previous reports and adapted to this study by performing preliminary studies to determine the appropriate non-cytotoxic range suitable for HPMCs.

Though treatment with both the small molecule inhibitor, JQ1, and the PROTAC, ARV-825 resulted in significant attenuation of MesoMT, ARV-825 showed more potent inhibition at as low as 5 nM while JQ1 began showing significant inhibition at 0.5 μ M and above, which suggests that ARV-825 is approximately one hundred-fold more effective than JQ1. This indicates that ARV-825 might be a more effective option for the pharmaceutical inhibition of BRD4. This more effective inhibition by ARV-825 over JQ1 might be explained by their mechanisms of action. Where the JQ1 competitively binds BRD4's acetyl-lysine recognition site and hinders the interactions by which BRD4 performs its functions [27], ARV-825 not only binds competitively but also enables the ubiquitin degradation of BRD4 by recruiting a ubiquitin ligase [28]. Thus, while BRD4 might have some other interactions that are not inhibited by the competitive binding of JQ1, its rapid ubiquitin-mediated degradation by the PROTAC eliminates any unknown interactions that could result in BRD4 induction, and by extension, MesoMT induction. The effect of ARV-825 is also more potent than JQ1 in inhibiting the cell proliferation of different cancer cells such as breast cancer cells [28] and gastric cancer cells [48].

More so, JQ1 is a pan-BD inhibitor, specific for all BET proteins, that is, it could bind either of the bromodomains (BDs) on any of the BET proteins. This indicates that it is not exclusively specific for BRD4 binding but also for BRD2 and BRD3. However, siRNA specific for BRD4 showed consistent effects as that of JQ1 and ARV-825, supporting a critical role of BRD4 in MesoMT. In addition, the binding affinity of JQ1 to different BDs varies. JQ1 has K_d values of approximately 50 nM and 90 nM for BD1 and BD2 binding, respectively, suggesting it has a higher binding affinity for BD1. [49].

Whether the BD-selective inhibitors have similar or different effects as pan-BD inhibitors in blocking/reversing MesoMT remains to be tested in the future.

On the other hand, ARV-825 has K_d values of 90 and 28 nM for BD1 and BD2 of BRD4, respectively. Which suggests that, unlike JQ1, ARV-825 has a higher binding affinity for BD2, and probably binds BD2 [50]. ARV-825 IC₅₀ values vary depending on the cells being considered, however, this might not have far-reaching consequences as, unlike JQ1, the overall mechanism of action of the PROTAC molecule overrides this effect in that brings about proteasomal degradation of BRD4, making the ARV-825 still more potent than the JQ1.

Furthermore, reversal inhibition studies were performed to test if pharmaceutical inhibition of BRD4 can reverse the established MesoMT using the JQ1 inhibitor. Reverse inhibition studies have more clinical relevance because they better represent the mode of disease development and therapeutic intervention in the clinic. In reversal studies, MesoMT was induced first, before the inhibitor treatment. Also in physiological conditions, the MesoMT process occurs first leading to PF before drug intervention meaning it takes the same mode of occurrence as the reverse inhibition. Western blot images (Figure 6) showed less attenuation in the expression of MesoMT markers compared to the effect of the JQ1 blockade inhibition (Figure 3A) suggesting that JQ1 reverses the induction of TGF- β -MesoMT in pleural cells but not as well effectively as it blocks the induction. In future investigations, we would like to compare reversal inhibition studies of ARV-825 to the effects of its blockade inhibition of BRD4 to see if it shows the same trend as JQ1 inhibition or otherwise. This might help in determining or

reinforcing which of the drugs is a better therapeutic option. In CCl₄-induced hepatic fibrosis, JQ1 was also shown to reverse or at least prevent the progression of liver fibrosis, but the effect of the reversal was not as dramatic as that in the blockade study [32].

The results obtained so far in this study suggest that BRD4 might represent a promising therapeutic target for blocking the induction of pleural MesoMT. In future studies, we will determine whether targeting BRD4 is effective in blocking or reversing the induction of PF using an experimental PF model induced by *Strep* that is clinically relevant. In view of this, some preliminary experiments have been performed to investigate the induction of BRD4 in a *Strep* model of pleural injury. The data (Figure 7) showed that *Strep* induced thickening of the pleural layer in C56BL/6 mice, indicating the development of PF. IHC staining using BRD4-specific antibody also revealed a strong BRD4 expression in the thickened pleura of mice challenged with *Strep*. This suggests the involvement of BRD4 in the induction of PF using the *Strep* model of pleural injury. This is similar to the upregulation of BRD4 observed in renal tissues of hypertensive nephropathy patients, a condition that leads to renal interstitial fibrosis [42] and in pathologic specimens from patients with liver fibrosis [51]. This creates a good foundation for further investigations of the therapeutic targeting of BRD4 in preclinical models of PF. Future work is also needed to define the mechanisms underlying BRD4 targeting in blocking pleural MesoMT.

This thesis has significant clinical relevance as it explores the potential of a novel mediator of MesoMT, BRD4, as a therapeutic target in the treatment of PF. Having

shown strong evidence of its potential *in vitro*, and some preliminary data *in vivo*, the study shows some potential to be an important contribution to what might be the answer in designing new and more effective therapeutic options in the treatment of PF.

REFERENCES

1. Weiskirchen, R., S. Weiskirchen, and F. Tacke, *Organ and tissue fibrosis: Molecular signals, cellular mechanisms and translational implications*. Mol Aspects Med, 2019. **65**: p. 2-15.
2. Henderson, N.C., F. Rieder, and T.A. Wynn, *Fibrosis: from mechanisms to medicines*. Nature, 2020. **587**(7835): p. 555-566.
3. Wynn, T.A., *Fibrotic disease and the TH1/TH2 paradigm*. Nature Reviews Immunology, 2004. **4**(8): p. 583-594.
4. Chanda, D., et al., *Developmental pathways in the pathogenesis of lung fibrosis*. Mol Aspects Med, 2019. **65**: p. 56-69.
5. Huggins, J.T. and S.A. Sahn, *PLEURAL EFFUSIONS | Pleural Fibrosis*, in *Encyclopedia of Respiratory Medicine*, G.J. Laurent and S.D. Shapiro, Editors. 2006, Academic Press: Oxford. p. 382-388.
6. Tucker, T.A. and S. Idell, *Update on Novel Targeted Therapy for Pleural Organization and Fibrosis*. Int J Mol Sci, 2022. **23**(3).
7. Huggins, J.T. and S.A. Sahn, *Causes and management of pleural fibrosis*. Respirology, 2004. **9**(4): p. 441-7.
8. Mutsaers, S.E., *The mesothelial cell*. Int J Biochem Cell Biol, 2004. **36**(1): p. 9-16.
9. Batra, H. and V.B. Antony, *Pleural mesothelial cells in pleural and lung diseases*. J Thorac Dis, 2015. **7**(6): p. 964-80.
10. Jantz, M.A. and V.B. Antony, *Pathophysiology of the pleura*. Respiration, 2008. **75**(2): p. 121-33.
11. Mutsaers, S.E., et al., *Pathogenesis of pleural fibrosis*. Respirology, 2004. **9**(4): p. 428-40.

12. Gordillo, C.H., et al., *Mesothelial-to-Mesenchymal Transition Contributes to the Generation of Carcinoma-Associated Fibroblasts in Locally Advanced Primary Colorectal Carcinomas*. *Cancers (Basel)*, 2020. **12**(2).
13. Logan, R., et al., *TGF- β regulation of the uPA/uPAR axis modulates mesothelial-mesenchymal transition (MesoMT)*. *Sci Rep*, 2021. **11**(1): p. 21210.
14. Tucker, T., et al., *Myocardin Is Involved in Mesothelial-Mesenchymal Transition of Human Pleural Mesothelial Cells*. *Am J Respir Cell Mol Biol*, 2019. **61**(1): p. 86-96.
15. Owens, S., et al., *Mesomesenchymal transition of pleural mesothelial cells is PI3K and NF- κ B dependent*. *Am J Physiol Lung Cell Mol Physiol*, 2015. **308**(12): p. L1265-73.
16. Pardali, E., et al., *TGF- β -Induced Endothelial-Mesenchymal Transition in Fibrotic Diseases*. *Int J Mol Sci*, 2017. **18**(10).
17. Hsieh, C.Y., et al., *Thrombin Upregulates PAI-1 and Mesothelial-Mesenchymal Transition Through PAR-1 and Contributes to Tuberculous Pleural Fibrosis*. *Int J Mol Sci*, 2019. **20**(20).
18. Qian, G., et al., *DOCK2 Promotes Pleural Fibrosis by Modulating Mesothelial to Mesenchymal Transition*. *Am J Respir Cell Mol Biol*, 2022. **66**(2): p. 171-182.
19. Zeng, L. and M.M. Zhou, *Bromodomain: an acetyl-lysine binding domain*. *FEBS Lett*, 2002. **513**(1): p. 124-8.
20. Dey, A., et al., *Brd4 marks select genes on mitotic chromatin and directs postmitotic transcription*. *Mol Biol Cell*, 2009. **20**(23): p. 4899-909.
21. Toyama, R., et al., *Brd4 associates with mitotic chromosomes throughout early zebrafish embryogenesis*. *Dev Dyn*, 2008. **237**(6): p. 1636-44.
22. Donati, B., E. Lorenzini, and A. Ciarrocchi, *BRD4 and Cancer: going beyond transcriptional regulation*. *Mol Cancer*, 2018. **17**(1): p. 164.
23. Hajmirza, A., et al., *BET Family Protein BRD4: An Emerging Actor in NF κ B Signaling in Inflammation and Cancer*. *Biomedicines*, 2018. **6**(1).
24. Stratton, M.S., S.M. Haldar, and T.A. McKinsey, *BRD4 inhibition for the treatment of pathological organ fibrosis*. *F1000Res*, 2017. **6**.
25. Liang, Y., J. Tian, and T. Wu, *BRD4 in physiology and pathology: "BET" on its partners*. *Bioessays*, 2021. **43**(12): p. e2100180.
26. Schwalm, M.P. and S. Knapp, *BET bromodomain inhibitors*. *Curr Opin Chem Biol*, 2022. **68**: p. 102148.
27. Shi, X., et al., *JQ1: a novel potential therapeutic target*. *Pharmazie*, 2018. **73**(9): p. 491-493.
28. Noblejas-López, M.D.M., et al., *Activity of BET-proteolysis targeting chimeric (PROTAC) compounds in triple negative breast cancer*. *J Exp Clin Cancer Res*, 2019. **38**(1): p. 383.

29. Wu, S., et al., *BRD4 PROTAC degrader ARV-825 inhibits T-cell acute lymphoblastic leukemia by targeting 'Undruggable' Myc-pathway genes*. *Cancer Cell Int*, 2021. **21**(1): p. 230.
30. Yang, T., et al., *A BRD4 PROTAC nanodrug for glioma therapy via the intervention of tumor cells proliferation, apoptosis and M2 macrophages polarization*. *Acta Pharm Sin B*, 2022. **12**(6): p. 2658-2671.
31. Song, S., et al., *Inhibition of BRD4 attenuates transverse aortic constriction- and TGF- β -induced endothelial-mesenchymal transition and cardiac fibrosis*. *J Mol Cell Cardiol*, 2019. **127**: p. 83-96.
32. Ding, N., et al., *BRD4 is a novel therapeutic target for liver fibrosis*. *Proc Natl Acad Sci U S A*, 2015. **112**(51): p. 15713-8.
33. Vichaikul, S., et al., *Inhibition of bromodomain extraterminal histone readers alleviates skin fibrosis in experimental models of scleroderma*. *JCI Insight*, 2022. **7**(9).
34. Xiong, C., et al., *Pharmacological targeting of BET proteins inhibits renal fibroblast activation and alleviates renal fibrosis*. *Oncotarget*, 2016. **7**(43): p. 69291-69308.
35. Yin, J., B. Han, and Y. Shen, *LncRNA NEAT1 inhibition upregulates miR-16-5p to restrain the progression of sepsis-induced lung injury via suppressing BRD4 in a mouse model*. *Int Immunopharmacol*, 2021. **97**: p. 107691.
36. Sanders, Y.Y., et al., *Brd4-p300 inhibition downregulates Nox4 and accelerates lung fibrosis resolution in aged mice*. *JCI Insight*, 2020. **5**(14).
37. Pooladanda, V., et al., *BRD4 targeting nanotherapy prevents lipopolysaccharide induced acute respiratory distress syndrome*. *Int J Pharm*, 2021. **601**: p. 120536.
38. Brasier, A.R. and J. Zhou, *Validation of the epigenetic reader bromodomain-containing protein 4 (BRD4) as a therapeutic target for treatment of airway remodeling*. *Drug Discov Today*, 2020. **25**(1): p. 126-132.
39. Kaneshita, S., et al., *CG223, a novel BET inhibitor, exerts TGF- β 1-mediated antifibrotic effects in a murine model of bleomycin-induced pulmonary fibrosis*. *Pulm Pharmacol Ther*, 2021. **70**: p. 102057.
40. Tang, X., et al., *Assessment of Brd4 inhibition in idiopathic pulmonary fibrosis lung fibroblasts and in vivo models of lung fibrosis*. *Am J Pathol*, 2013. **183**(2): p. 470-9.
41. Qin, W., et al., *NOX1 Promotes Mesothelial-Mesenchymal Transition through Modulation of Reactive Oxygen Species-mediated Signaling*. *Am J Respir Cell Mol Biol*, 2021. **64**(4): p. 492-503.
42. Wang, X., et al., *Bromodomain-containing protein 4 contributes to renal fibrosis through the induction of epithelial-mesenchymal transition*. *Experimental Cell Research*, 2019. **383**(2): p. 111507.

43. Mu, J., et al., *BRD4 inhibition by JQ1 prevents high-fat diet-induced diabetic cardiomyopathy by activating PINK1/Parkin-mediated mitophagy in vivo*. *J Mol Cell Cardiol*, 2020. **149**: p. 1-14.
44. Shim, J.M., et al., *BET proteins are a key component of immunoglobulin gene expression*. *Epigenomics*, 2017. **9**(4): p. 393-406.
45. Li, Y., et al., *Inhibition of Brd4 by JQ1 Promotes Functional Recovery From Spinal Cord Injury by Activating Autophagy*. *Front Cell Neurosci*, 2020. **14**: p. 555591.
46. Cooper, J.M., et al., *Overcoming BET Inhibitor Resistance in Malignant Peripheral Nerve Sheath Tumors*. *Clin Cancer Res*, 2019. **25**(11): p. 3404-3416.
47. Lam, F.C., et al., *BRD4 prevents the accumulation of R-loops and protects against transcription-replication collision events and DNA damage*. *Nat Commun*, 2020. **11**(1): p. 4083.
48. Liao, X., et al., *ARV-825 Demonstrates Antitumor Activity in Gastric Cancer via MYC-Targets and G2M-Checkpoint Signaling Pathways*. *Front Oncol*, 2021. **11**: p. 753119.
49. Filippakopoulos, P., et al., *Selective inhibition of BET bromodomains*. *Nature*, 2010. **468**(7327): p. 1067-73.
50. Lu, J., et al., *Hijacking the E3 Ubiquitin Ligase Cereblon to Efficiently Target BRD4*. *Chem Biol*, 2015. **22**(6): p. 755-63.
51. Wu, C., et al., *Hepatic BRD4 Is Upregulated in Liver Fibrosis of Various Etiologies and Positively Correlated to Fibrotic Severity*. *Front Med (Lausanne)*, 2021. **8**: p. 683506.

VITA

Joy Adewumi entered the Obafemi Awolowo University, Nigeria, as an undergraduate student in 2015 majoring in biochemistry. She graduated with a Bachelor of Science degree in Biochemistry in July 2019. In August 2021, she joined the Biotechnology Graduate Program at the University of Texas at Tyler Health Science Center where she completed her thesis work in the lab of Dr. Guoqing Qian. After graduation, Joy plans to join a PhD program in a relevant field to further pursue a career in science and biotechnology.

This thesis was typed by Joy Adewumi.